

AD-A283 142



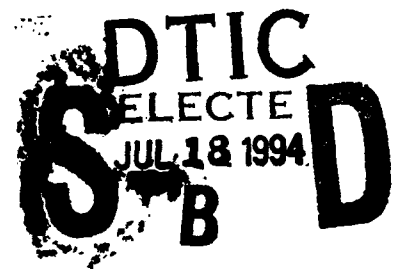
PL-TR-94-2005

**NONLINEAR HYSTERESIS
IN AN ENDOCHRONIC SOLID****Jean-Bernard Minster**

University of California, San Diego
Scripps Institution of Oceanography, A-025
Institute of Geophysics and Planetary Physics
La Jolla, CA 92093-0225

4 January 1994

Final Report
1 November 1988-3 November 1993

Approved for public release; distribution unlimited

PHILLIPS LABORATORY
Directorate of Geophysics
AIR FORCE MATERIEL COMMAND
HANSCOM AIR FORCE BASE, MA 01731-3010

94-22403

2988

DTIC QUALITY INSPECTED 1


94 7 15 040


SPONSORED BY
Advanced Research Projects Agency (DoD)
Nuclear Monitoring Research Office
ARPA ORDER NO 5299

MONITORED BY
Phillips Laboratory
CONTRACT NO. F19628-88-K-0039

The views and conclusions contained in this document are those of the authors and should not be interpreted as representing the official policies, either express or implied, of the Air Force or the U.S. Government.

This technical report has been reviewed and is approved for publication.


JAMES F. LEWKOWICZ
Contract Manager
Solid Earth Geophysics Branch
Earth Sciences Division


JAMES F. LEWKOWICZ
Branch Chief
Solid Earth Geophysics Branch
Earth Sciences Division


JAMES F. LEWKOWICZ, Acting Director
Earth Sciences Division

This report has been reviewed by the ESC Public Affairs Office (PA) and is releasable to the National Technical Information Service (NTIS).

Qualified requestors may obtain additional copies from the Defense Technical Information Center. All others should apply to the National Technical Information Service.

If your address has changed, or if you wish to be removed from the mailing list, or if the addressee is no longer employed by your organization, please notify PL/TSL, 29 Randolph Road, Hanscom AFB, MA 01731-3010. This will assist us in maintaining a current mailing list.

Do not return copies of this report unless contractual obligations or notices on a specific document requires that it be returned.

REPORT DOCUMENTATION PAGE			Form Approved OMB No. 0704-0188	
Public reporting burden for this collection of information is estimated to average 1 hour per response, including the time for reviewing instructions, searching existing data sources, gathering and maintaining the data needed, and completing and reviewing the collection of information. Send comments regarding this burden estimate or any other aspect of this collection of information, including suggestions for reducing this burden to Washington Headquarters Services, Directorate for Information Operations and Reports, 1215 Jefferson Davis Highway, Suite 1204 Arlington, VA 22202-4302, and to the Office of Management and Budget, Paperwork Reduction Project (0704-0188) Washington, D.C. 20503.				
1. AGENCY USE ONLY (Leave blank)		2. REPORT DATE 4 January 1994		3. REPORT TYPE AND DATES COVERED Final Technical Report, 11/1/88-11/3/93
4. TITLE AND SUBTITLE NONLINEAR HYSTERESIS IN AN ENDOCHRONIC SOLID			5. FUNDING NUMBERS PE 62714 E PR 8A10 TA DA WUAR Contract # F19628-88-K-0039	
6. AUTHOR(S) Jean-Bernard Minster				
7. PERFORMING ORGANIZATION NAME(S) AND ADDRESS(ES) The Regents of the University of California Scripps Institution of Oceanography IGPP 0225, 9500 Gilman Drive La Jolla, California 92093-0225			8. PERFORMING ORGANIZATION REPORT NUMBER	
9. SPONSORING/MONITORING AGENCY NAME(S) AND ADDRESS(ES) Phillips Laboratory 29 Randolph Road Hanscom AFB, MA 01731-3010 Contract Manager: James F. Lewkowicz/GPEH			10. SPONSORING /MONITORING AGENCY REPORT NUMBER PL-TR-94-2005	
11. SUPPLEMENTARY NOTES This research was also supported by DOE, under LLNL contract no. B157346, and LLNL UC Master Task Agreement Task # 4				
12a. DISTRIBUTION/AVAILABILITY STATEMENT Approved for public release, distribution unlimited			12b. DISTRIBUTION CODE	
13. ABSTRACT (Maximum 200 words) Propagation of seismic waves in the nearfield where rock rheology is demonstrably nonlinear raises unique difficulties. Nonlinearity arises primarily in two forms at intermediate to large strains: (1) nonlinear elasticity, and (2) amplitude-dependent attenuation. The proper representation of nonlinear constitutive equations for rocks in this regime is a potentially important ingredient of quantitative source models. We have shown previously that nonlinear one-dimensional wave propagation can result in spectral distortions at all wavelengths. This effect is strongly pulse-shape dependent, and therefore calls for 3-D capability. More recently, we found that our approximate description of the phenomenology in the nonlinear regime was inadequate and unable to simulate new laboratory observations. We describe an intrinsically nonlinear rheological model, based on the endochronic framework of K. Valanis, which replicates the main features of observed hysteresis loops in the strain regime of interest and is easily reduced to differential form. The resulting differential equations can be readily solved numerically. Thus, this model is suitable for finite difference and finite element stress wave codes. Ultimately, a complete description of the rheology in terms of a thermodynamically valid constitutive equation is really what should be used in numerical simulations, if it can be developed and validated experimentally.				
14. SUBJECT TERMS Rock mechanics, nonlinear rheology, source medium properties			15. NUMBER OF PAGES 34	
			16. PRICE CODE	
17. SECURITY CLASSIFICATION OF REPORT unclassified	18. SECURITY CLASSIFICATION OF THIS PAGE unclassified	19. SECURITY CLASSIFICATION OF ABSTRACT unclassified	20. LIMITATION OF ABSTRACT SAR	

Table of Contents

1.	INTRODUCTION.....	1
2.	NONLINEAR WAVE PROPAGATION AND ATTENUATION.....	1
3.	LABORATORY OBSERVATIONS OF HYSTERESIS LOOPS	3
4.	ENDOCHRONIC CONSTITUTIVE MODEL.....	9
4.1	<i>Introduction</i>	9
4.2	<i>Background to the Endochronic Formulation</i>	9
4.3	<i>The Endochronic Material Model</i>	9
4.4	<i>Amplitude-Dependence of Q in the Endochronic Model</i>	10
4.5	<i>Computational approach</i>	10
5.	APPLICATION TO LABORATORY AND FIELD DATA	11
6.	CONCLUSIONS.....	16
	REFERENCES.....	17

Accession For	
NTIS GRA&I	<input checked="" type="checkbox"/>
DTIC TAB	<input type="checkbox"/>
Unannounced	<input type="checkbox"/>
Justification	
By	
Distribution/	
Availability Codes	
Dist	Avail and/or Special
A-1	

Summary

Propagation of seismic waves in the nearfield where rock rheology is demonstrably nonlinear raises unique difficulties. Nonlinearity arises primarily in two forms at intermediate to large strains: (1) nonlinear elasticity, and (2) amplitude-dependent attenuation. The proper representation of nonlinear constitutive equations for rocks in this regime is a potentially important ingredient of quantitative source models.

We have shown previously that nonlinear one-dimensional wave propagation can result in spectral distortions at all wavelengths. This effect is strongly pulse-shape dependent, and therefore calls for a 3-D capability. More recently, we found that our approximate description of the phenomenology in the nonlinear regime was inadequate and unable to simulate new laboratory observations. We describe an intrinsically nonlinear rheological model, based on the endochronic framework of K. Valanis, which replicates the main features of observed hysteresis loops in the strain regime of interest and is easily reduced to differential form. The resulting differential equations can be readily solved numerically. Thus, this model is suitable for finite difference and finite element stress wave codes. Ultimately, a complete description of the rheology in terms of a thermodynamically valid constitutive equation is really what should be used in numerical simulations, if it can be developed and validated experimentally.

This research was also supported by DOE, under LLNL Contract No. B157346, and LLNL UC Master Task Agreement, Task #4.

Acknowledgments

This research was supported by DARPA contract F19628-88-K-0039, and monitored by the Department of the Air Force, Phillips Laboratory (AF/PL), and under the auspices of the Department of Energy, Office of Research and Development, through the Lawrence Livermore National Laboratory, Project No. ST-364. Data used in this paper have been collected by New England Research Inc., and have been kindly made available to us by Drs. R. Martin, R. Haupt, and G. Boitnott. We thank Drs. B. Bonner of LLNL, P.A. Johnson and K.R. McCall of LANL for interesting and informative discussions.

Nonlinear Hysteresis in an Endochronic Solid

Steven M. Day

San Diego State University, San Diego, CA

Jean-Bernard Minster, Michael Tryon, and Lois Yu

Scripps Institution of Oceanography, IGPP, La Jolla, CA 92093

1. INTRODUCTION

Propagation of seismic waves in the nearfield where rock rheology is demonstrably nonlinear raises unique difficulties. Nonlinearity arises primarily in two forms at intermediate to large strains: (1) nonlinear elasticity, and (2) amplitude-dependent attenuation, which is a well documented behavior at intermediate strains and low confining pressure. The proper representation of nonlinear constitutive equations for rocks in this regime is a potentially important ingredient of quantitative source models.

Stress wave propagation and attenuation, in rocks and soils, show evidence of significant nonlinearity at strain amplitudes as low as 10^{-6} , leading in particular to an amplitude dependence of the apparent Q , most likely associated with friction along microcracks and joints [e.g. *Boitnott*, 1992]. Recent quasistatic laboratory testing of rock at low strain has permitted detailed high-quality observations of cusped hysteresis loops in this regime. These issues have been recently reviewed by *Minster et al.* [1991] and summarized by *Martin and Minster* [1992]. Nonlinear wave propagation in geological materials has also been observed and modeled in a different context by *Bonner and Wannamaker* [1991], and by *Johnson et al.* [1991]. Our objective is to identify and validate a rheological model (constitutive equation) for rocks, valid at moderate strains, that explains satisfactorily these various observations, and is appropriate for incorporation in numerical source and wave propagation codes, and apply the rheological model to improve our understanding of seismic source physics.

We have shown in previous work that nonlinear one-dimensional wave propagation can result in spectral distortions at all wavelengths, but that this effect is strongly pulse-shape dependent, and therefore call for a 3-D capability [*Minster et al.*, 1991]. More recently, we have found that our use of an approximate description of the phenomenological behavior of rocks in the nonlinear regime is flawed insofar as it is not able to simulate new high-quality laboratory observations of hysteresis loops in both Sierra White granite and Berea sandstone [*Day et al.*, 1992]. Ultimately, a complete description of the rheology in terms of a thermodynamically valid constitutive equation is really what should be used in numerical simulations, if it can be developed and validated experimentally.

2. NONLINEAR WAVE PROPAGATION AND ATTENUATION

Our earlier numerical modeling of nonlinear attenuation in the intermediate strain regime used viscoelastic theory as its point of departure [*Minster and Day*, 1986; *Minster et al.* 1991]. We review that approach here, in order to highlight its analogies as well as its contrasts with the new approach proposed in Section 4. A further reason for reviewing the numerical approach to viscoelasticity is that, to be acceptable, a model for the nonlinear intermediate strain regime should be well behaved in the low strain limit. Thus, it will be desirable to develop a numerical wave propagation treatment which reduces to linear viscoelasticity in the small amplitude limit.

Based on a suite of one-dimensional simulations of nonlinear wave propagation problems *Minster et al.* [1991] concluded that a simple model in which Q^{-1} is simply assumed to be proportional to strain amplitude can explain the shape distortion of Lorentz peaks observed in the laboratory at moderate strains, and the apparent superposability of simple pulses even in the nonlinear regime. They also concluded that, in contrast to linear Q models for which the spectrum of the “ Q operator” tends to unity at low frequencies, a nonlinear rheology may lead to significant spectral distortions *at all frequencies*, and energy losses can be substantial even at wavelengths long compared to the propagation distance. Thus, even though nonlinear rheology is only relevant within a limited distance from a seismic source, this raises the possibility that the far field source spectrum can be affected to some degree at all frequencies, including those pertinent to regional phases and teleseismic body waves.

Those results were based on an attenuation model described by

$$Q^{-1} = Q_a^{-1} + \gamma \epsilon, \quad (2.1)$$

where ϵ is the strain amplitude, γ is a material constant, and Q_a^{-1} represents a linear anelastic term controlled by mechanisms that mask the nonlinear ones at low strain. This form of amplitude-dependence describes well the bulk of laboratory evidence accumulated to date. Nonlinear wave propagation simulations were conducted in two steps. First, we used the Padé approximant method of *Day and Minster* [1984] to convert the stress-strain relation of a linear, anelastic solid, with frequency-independent Q , into differential form. An absorption band, with Q nearly constant at Q_0 , and with minimum and maximum relaxation times τ_1 and τ_2 , respectively, yields the following relation between stress history, $\sigma(t)$ and strain history, $\epsilon(t)$

$$\sigma(t) = \int_0^t M_u \left[1 - \frac{2}{\pi Q_0} \int_{\tau_1}^{\tau_2} (1 - e^{-(t-t')/\tau}) \frac{d\tau}{\tau} \right] d\epsilon(t'), \quad (2.2)$$

where M_u is the unrelaxed modulus. We showed that (2.2) can be approximated by

$$\sigma(t) = M_u \left[\epsilon(t) - \sum_{i=1}^n \zeta_i(t) \right], \quad (2.3)$$

where the ζ_i 's are relaxation terms governed by the n linear equations

$$\frac{d\zeta_i}{dt} + \nu_i \zeta_i = \frac{\tau_1^{-1} - \tau_2^{-1}}{\pi} w_i Q_0^{-1} \epsilon(t), \quad (2.4)$$

The constants ν_i and w_i which depend on the order of approximation, n , are given by *Day and Minster* [1984], who also show that the operator defined by (2.3) and (2.4) converges to the exact result (2.2) as n increases. The second step is to generalize (2.4) by introducing a linear dependence of Q_0 on strain amplitude according to (2.1):

$$\frac{d\zeta_i}{dt} + \nu_i \zeta_i = \frac{\tau_1^{-1} - \tau_2^{-1}}{\pi} w_i (Q_a^{-1} + \gamma \epsilon(t)) \epsilon(t). \quad (2.5)$$

Then, (2.3) and (2.5) constitute the stress-strain equations for our one-dimensional finite difference simulations.

All differential operators generated by this procedure can be guaranteed to be causal, stable, and dissipative. However, that the method performs rather poorly when the

absorption band is much broader than the calculational pass band, that is, the interval between the maximum and minimum frequencies resolvable by the numerical method. For example, the finite difference method is limited to the frequency band from $1/n\delta t$ to roughly $1/m\delta t$, where δt is the time step, n is the total number of time steps computed, and m is the number of time steps associated with the minimum resolvable wavelength; m is typically of the order of 20, and n may be up to several thousand for large two-dimensional calculations. We have devised a simple extension of the method which renders it suitable for broad absorption bands, without compromising its analytical and numerical simplicity. Using the Laplace transform in s -multiplied form, we reduce the stress-strain relation to its operational form:

$$\bar{\sigma}(s) = \bar{M}(s) \bar{\epsilon}(s) \quad (2.6)$$

Note that the operational modulus \bar{M} has the same dimensions as the step response M . The unrelaxed modulus M_u , the relaxed modulus M_R , the modulus defect, δM , and the normalized relaxation function ϕ , are given by

$$M_u = M(0) = \bar{M}(\infty) \quad (2.7)$$

$$M_R = M(\infty) = \bar{M}(0) \quad (2.8)$$

$$\delta M = M_u - M_R \quad (2.9)$$

$$M(t) = M_R + \delta M \phi(t) \quad (2.10)$$

We represent the relaxation function in terms of a relaxation spectrum Φ ,

$$\phi(t) = \int_{-\infty}^{\infty} \Phi(\ln \tau) \exp(-t/\tau) d(\ln \tau) \quad (2.11)$$

resulting in the following integral expression for the operational modulus:

$$\bar{M}(s) = M_u - \delta M \int_0^{\infty} \frac{\hat{\Phi}(p) dp}{s + p} \quad (2.12)$$

where $\hat{\Phi}(p) = \Phi(\ln \tau^{-1})$. We may now partition of the p integral into 3 regimes, separated by low-frequency cutoff p_{min} and high-frequency cutoff p_{max}

$$\bar{M}(s) = M_u - \delta M (I_1 + I_2 + I_3) \quad (2.13)$$

$$I_1 = \int_0^{p_{min}} \frac{\hat{\Phi}(p) dp}{s + p} \quad I_2 = \int_{p_{min}}^{p_{max}} \frac{\hat{\Phi}(p) dp}{s + p} \quad I_3 = \int_{p_{max}}^{\infty} \frac{\hat{\Phi}(p) dp}{s + p} \quad (2.14, 15, 16)$$

The interval (p_{min}, p_{max}) is prescribed to coincide with the calculational pass band. The middle partition, I_2 , is replaced with an n^{th} order Padé approximant, as before, but with the support interval of interval of Φ , $(\tau_2^{-1}, \tau_1^{-1})$, replaced by the interval (p_{min}, p_{max}) . Then I_1 and I_3 are approximated by Taylor series about ∞ and 0, respectively. Laplace inversion leads to a representation of total stress as a sum of $n+2$ internal variables, each of which satisfies a first order differential equation. This permits us to model broad absorption bands efficiently and with much better accuracy than before.

3. LABORATORY OBSERVATIONS OF HYSTERESIS LOOPS

In order to validate the nonlinear models described above, we have conducted simulations of hysteresis loops measured at several strain amplitudes in uniaxial tests on Sierra White granite and Berea sandstone. These data have been collected by New England Research Inc., and have been kindly made available to us by Drs. R. Martin, R. Haupt, and G. Boitnott. As reported by *Day et al.* [1992], these simulations brought to light a serious shortcoming of our approach, namely that it does not produce the correct loop shapes when the strain amplitude is increased into the nonlinear regime. Various modifications of our general approach all resulted in failure, pointing to the need for a completely different treatment of the rheology, dealing *intrinsically* with the nonlinearity.

Laboratory stress-strain curves under cyclic loading characteristically exhibit the following features which a successful model must emulate:

- Hysteresis occurs, implying energy loss, and the effective Q characterizing this dissipation is strain-amplitude dependent.
- The hysteresis loops are cusped at reversal points, rather than elliptical (as would typify linear anelastic behavior).
- No yield surface is evident in the loading curves, at least for strains up to about 10^{-4} .
- Upon reversal of strain path, the tangent modulus is roughly equal to the instantaneous elastic modulus.

Typical raw laboratory data in the form of stress and strain histories are often rather noisy, and require filtering. Simple low-pass filtering smooths the cusps, thereby masking the onset of nonlinear behavior, and affecting the measurement of moduli at and near the cusps. We have therefore developed a technique to filter separately the loading and unloading portions of the loops. It relies on the construction of a longer time series out of a half-loop—that is a portion of stress-strain history between two reversals, in which both stress and strain are monotonic. This is done by extending it in both directions with versions of itself, rotated by $\pm\pi$ about its end points. The extended time series is then de-meant, de-trended, and low-pass filtered using a phaseless filter to avoid introduction of a phase shift. The filtered version is truncated to the original length after restoring trend and mean, and the stress-strain path reconstructed by concatenation of filtered segments. The rotation by $\pm\pi$ of the extensions has the advantage of preserving the continuity of the time series and its derivative, thereby limiting undesirable end effects. It is important to avoid introducing cusps into hysteresis loops when they are not present, and to avoid smoothing through a cusp or changing its angle, when one is present. Too strong a filter will change the slope near the end points, and therefore introduce a fictitious cusp. Misapplication of the technique is detectable because this will create overlaps or gaps between successive segments. The technique gives very satisfactory results for noise levels as large as 10 percent as we have been able to verify using synthetic loops contaminated with additive noise. This approach facilitates considerably the estimation of the tangent modulus, particularly near the loop ends where noise contamination is most worrisome.

Several of the features described above are evident in Figures 1 and 2, which show selected sequences of hysteresis loops in Berea Sandstone and in Sierra White, respectively, under uniaxial stress. In both instances, the strain and stress time histories are shown in the top frame, followed by the corresponding stress-strain paths (hysteresis loops) on an expanded scale, after removal of the mean slope, in order to emphasise the key nonlinear characteristics; the bottom frame illustrates the dependence of the tangent modulus on strain. In the filtered data, the cusped nature of the reversal points is evident. Also evident is the near-equality of the initial loading and unloading slopes. The results illustrate clearly the non-elliptical (nonlinear) character of the hysteresis loops at such moderate strain levels, and also bring out clearly the strain hardening which causes the loops to show upward concavity.

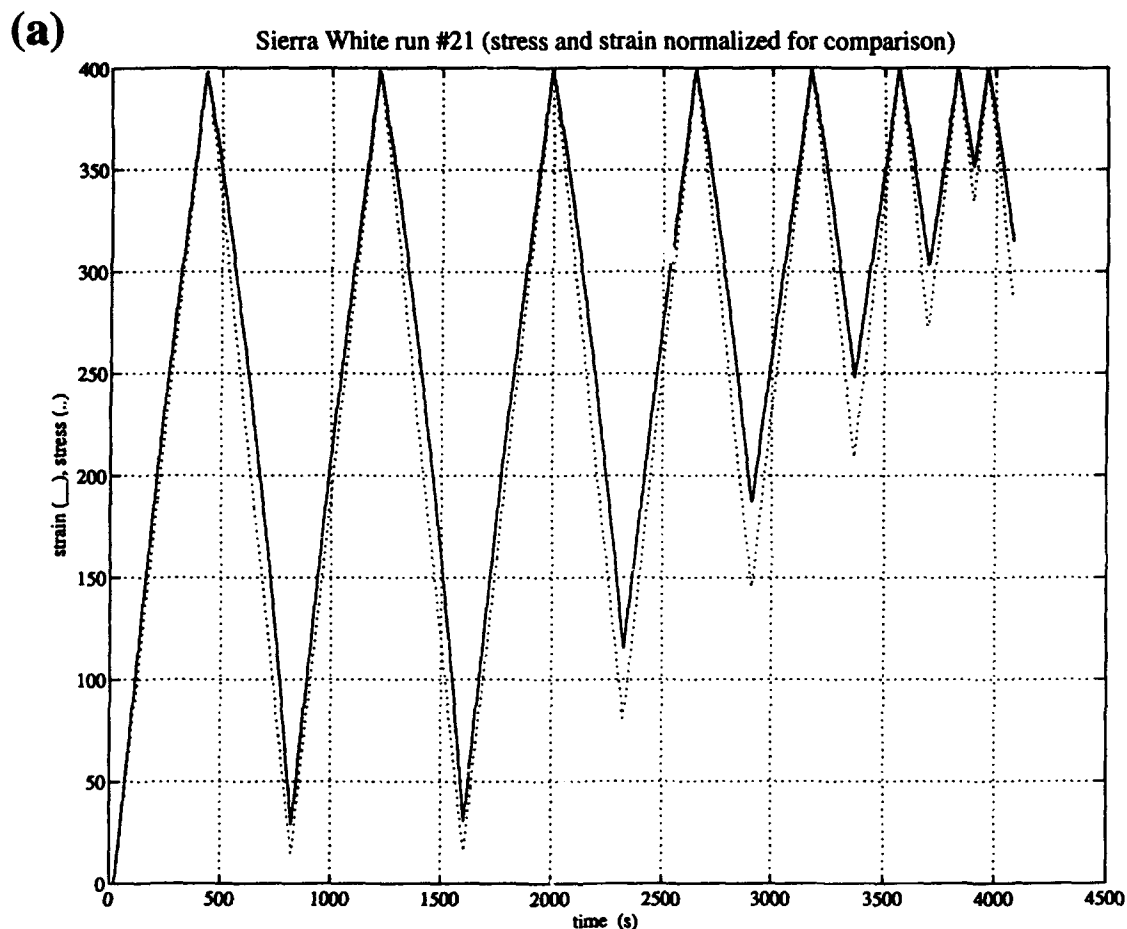


Figure 1: (a) Strain (solid line) and stress (dotted line) time histories for a uniaxial stress test on Sierra White granite. (b) corresponding stress and strain path, after smoothing; raw data are indicated by the dots, and the mean slope (modulus) of the hysteresis loops has been removed to emphasize the nonlinear characteristics. (c) Young's modulus dependence on strain for this test. Numbers indicate the various segments in the loading history, separated by path reversals.

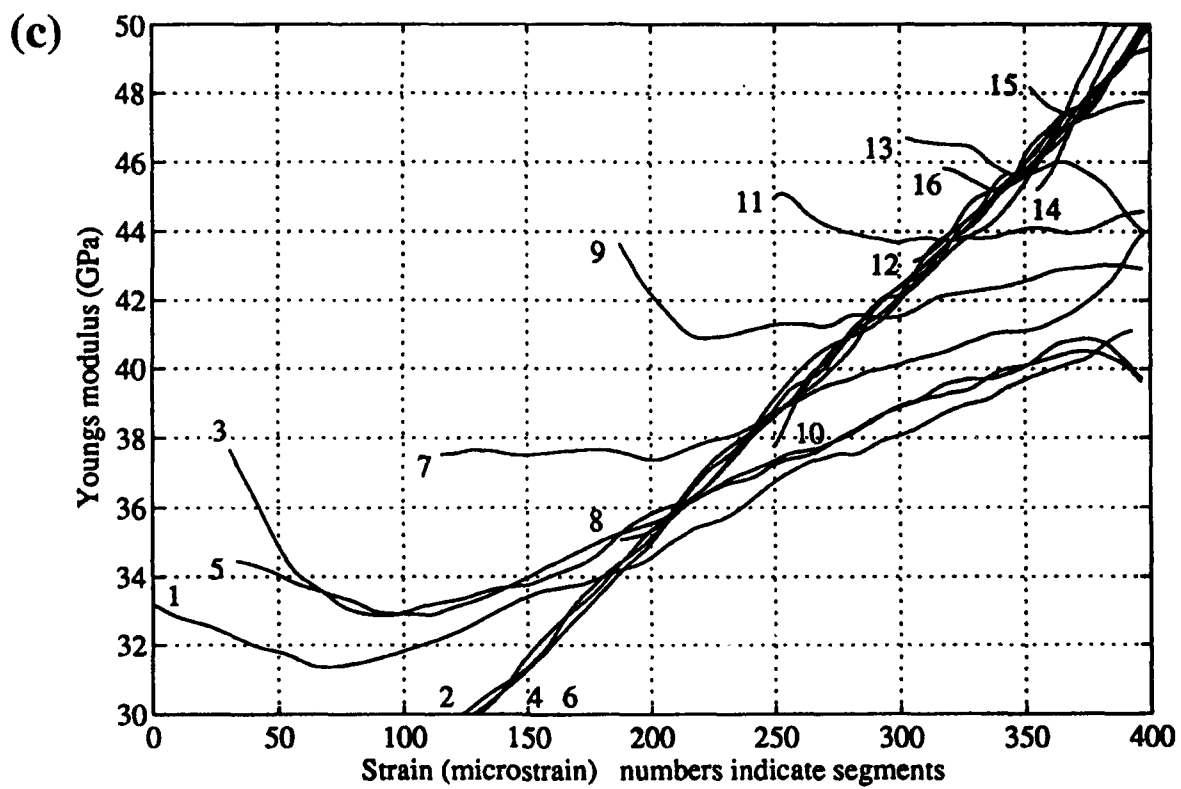
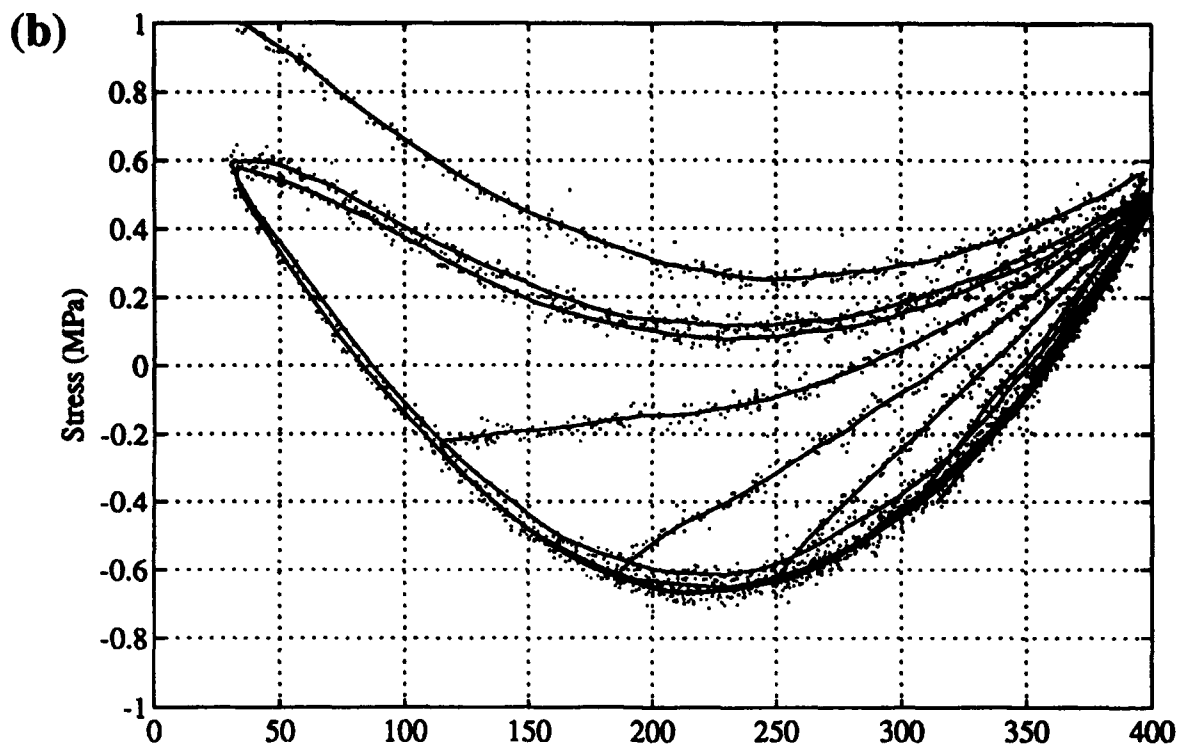


Figure 1. (continued)

(a)

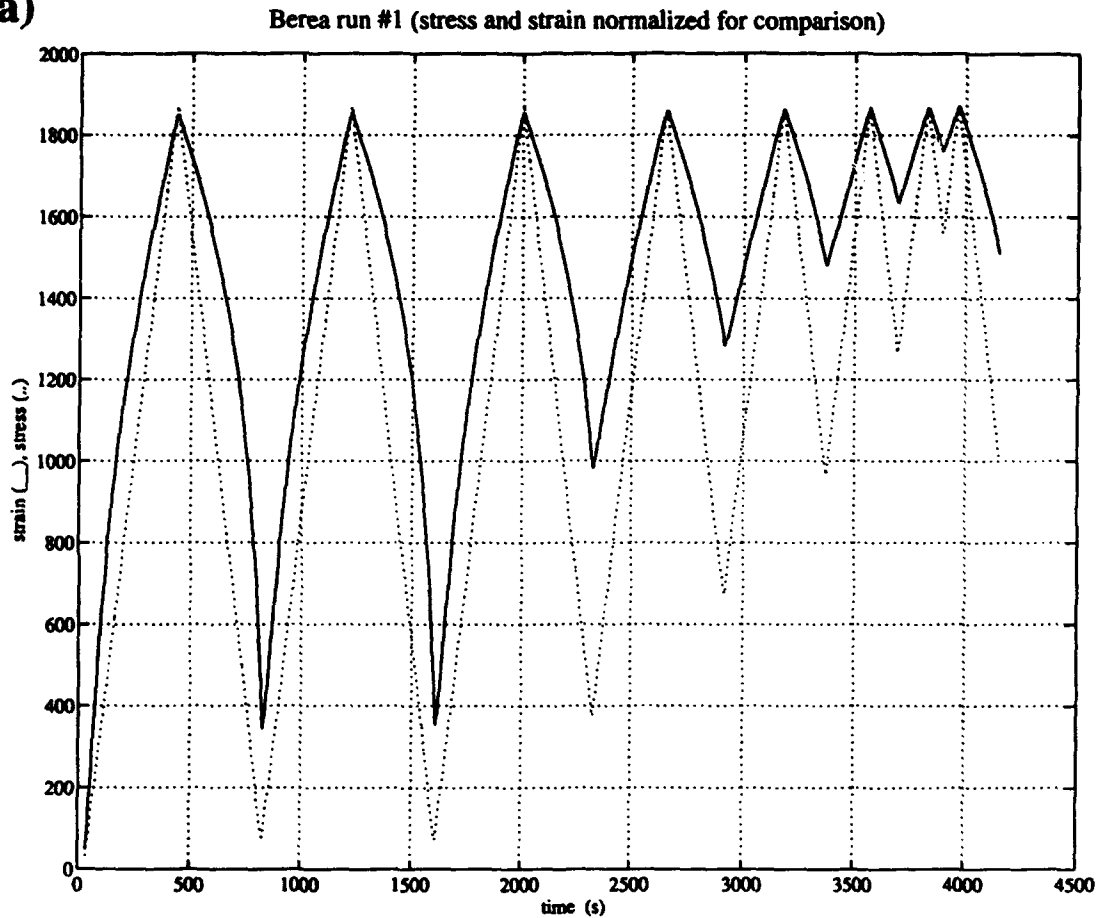


Figure 2: (a) Strain (solid line) and stress (dotted line) time histories for a uniaxial stress test on Berea Sandstone. (b) corresponding stress and strain path, after smoothing; raw data are indicated by the dots, and the mean slope (modulus) of the hysteresis loops has been removed to emphasize the nonlinear characteristics. (c) Young's modulus dependence on strain for this test. Numbers indicate the various segments in the loading history, separated by path reversals.

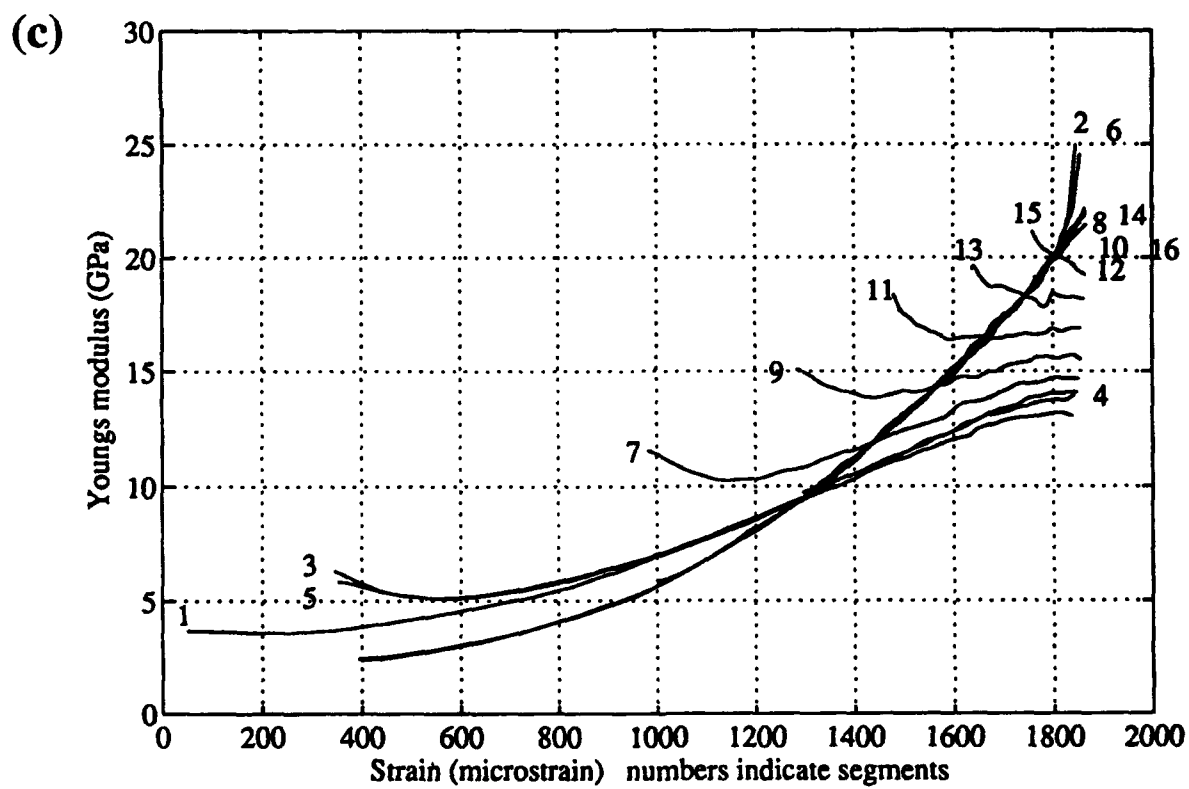
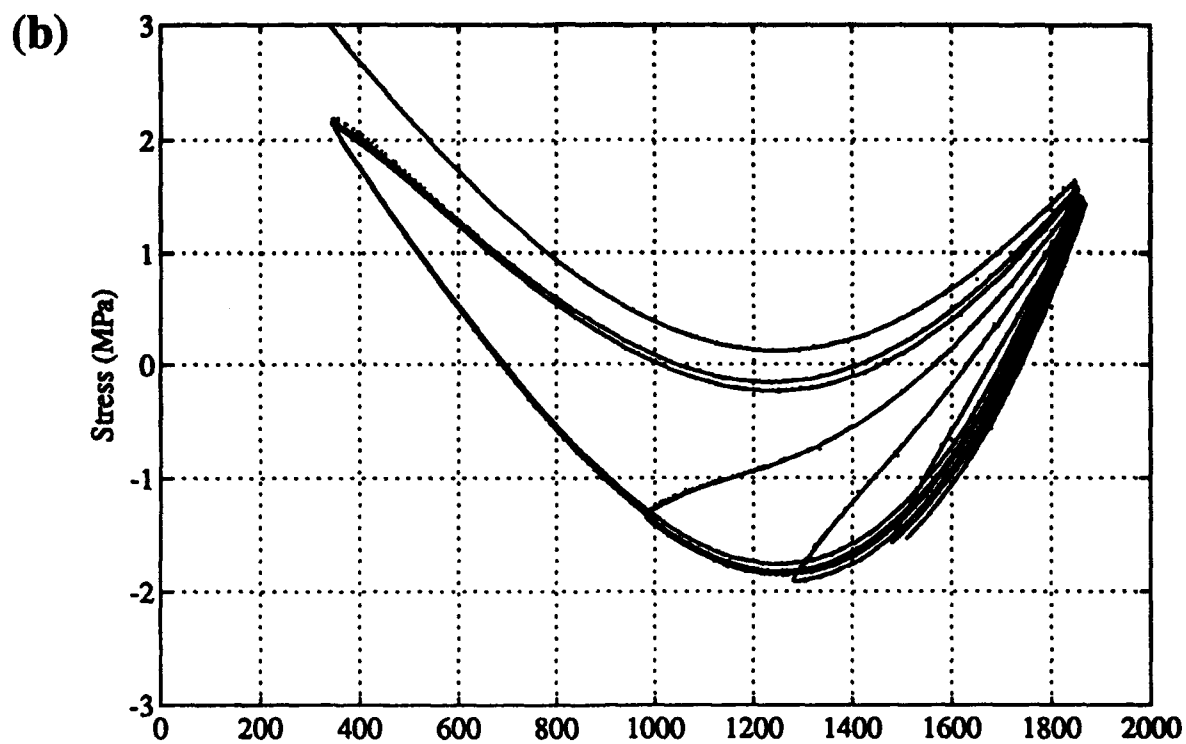


Figure 2. (continued)

4. ENDOCHRONIC CONSTITUTIVE MODEL

4.1 Introduction

A successful rheological model should be capable of matching the features seen in Figures 1 and 2, which are often difficult to see in the raw data, but it should, as much as possible, avoid introducing a large number of additional model parameters for this purpose. The endochronic model described in this paper offers, we think, a very promising solution. In light of the observations outlined in the previous section, we have adopted an approach to modeling the moderate strain regime which departs sharply from viscoelastic models, yet retains much of the computational simplicity described in Section 2.

4.2 Background to the Endochronic Formulation

From the outset, we consider the class of constitutive models known as *simple materials*. With this restriction, the stress at a point depends only on the strain history at that point (not, for example, on strain gradients), i. e.,

$$\sigma(t) = F[e(t'), 0 \leq t' \leq t], \quad (4.1)$$

where F is a functional relating the stress σ to the strain history $e(t)$. For example: if F is linear and time invariant, equation (1) reduces to a convolution, and we have the usual formulation of viscoelasticity:

$$\sigma(t) = M(t) * e(t), \quad (4.2)$$

This restriction combined with rate independence constitute sufficient conditions to ensure preservation of cube root scaling. To specialize 4.1 for a rate-independent simple material, we express the strain history in terms of the strain path length ξ . Then

$$\sigma(t) = F[e(\xi), \xi, 0 \leq \xi(t') \leq \xi(t)], \quad (4.3)$$

The concept of rate-independence implies that there is no dependence of the rheology on the rate $\dot{\xi}$:

$$\sigma(t) = F[e(\xi), 0 \leq \xi(t') \leq \xi(t)], \quad (4.4)$$

where

$$d\xi = (de:g:de)^{1/2}. \quad (4.5)$$

In other words, ξ is the strain path length, measured in terms of the metric g .

4.3 The Endochronic Material Model

Following Valanis and Read [1979], we consider the special case in which F is linear and shift-invariant in the *plastic* strain path length z

$$dz = (d\theta:g:d\theta)^{1/2} \quad (4.6)$$

where

$$d\theta = de - \frac{d\sigma}{2\mu} \quad (4.7)$$

is the plastic strain increment. The linear, shift-invariant assumption guarantees that we can write σ as a convolution over z ; that is:

$$\sigma(t) = K(z) * \frac{d\theta}{dz} \quad (4.8)$$

If the kernel $K(z)$ is chosen to have an integrable singularity at $z = 0$, then all the features noted above are realized:

$$K(z) \propto z^{-\alpha}, 0 < \alpha < 1. \quad (4.9)$$

It is the singular behavior of the kernel that insures that loading and unloading at reversal points occurs with stress-strain slope equal to the elastic modulus. Furthermore, as demonstrated below, we have been able to show that the singular kernel ensures power law dependence of Q^{-1} on strain amplitude, in accordance with experimental observations cited previously.

4.4 Amplitude-Dependence of Q in the Endochronic Model

The power law amplitude dependence of Q^{-1} is derived by noting that

$$\sigma \propto \int_0^z (z-z')^{-\alpha} \frac{d\theta(z')}{dz'} dz'. \quad (4.10)$$

Restricting treatment to uniaxial loading,

$$\left| \frac{d\theta}{dz} \right| = 1 \quad (4.11)$$

so, in terms of the maximum plastic strain z_m ,

$$\sigma \propto (z_m)^{1-\alpha}. \quad (4.12)$$

From the definition of Q^{-1} in terms of the area of the hysteresis loop, we obtain:

$$Q^{-1} \propto \frac{\sigma_m z_m}{\sigma_m^2}, \quad (4.13)$$

and from 4.13 and 4.14, we obtain

$$Q^{-1} \propto (\sigma_m)^{\alpha/(1-\alpha)}. \quad (4.14)$$

Note that for $\alpha = 1/2$, we have an approximately linear dependence on strain amplitude, in agreement with a large body of laboratory observations. The endochronic model thus appears capable of emulating laboratory observations of hysteretic behavior, as well as amplitude dependence of attenuation at moderate strain amplitudes.

4.5 Computational approach

To be useful for numerical simulations, the convolution form 4.8 must be converted to a differential constitutive equation. Since the endochronic model has a formal structure similar to linear viscoelasticity, we can carry out this conversion in a manner analogous to that used in Section 2. That is, we first Laplace transform 4.8,

$$\bar{\sigma}(s) = s \bar{K}(s) \bar{\theta}(s) \quad (4.15)$$

We approximate $\bar{K}(s)$ by a rational function $\bar{K}_n(s)$, where n is the order of the denominator. Then, we develop $\bar{K}_n(s)$ as a partial fraction expansion

$$\bar{K}_n(s) = \sum_{j=1}^n \frac{\lambda_j}{s + v_j}, \quad (4.16)$$

where v_j and λ_j are the poles and residues, respectively, of $\bar{K}_n(s)$.

Transformation back to the z domain yields the following system of differential equations for σ :

$$\sigma(z) = \sum_{j=1}^n \zeta_j$$

$$\frac{d\zeta_j(z)}{dz} + v_j \zeta_j(z) = \lambda_j \frac{d\theta}{dz}$$
(4.17)

Equations 4.6, 4.7, and 4.17 form the set of constitutive equations which are solved numerically. A convenient numerical scheme for the solution of such a system is given by *Murakami and Read* [1989], and we have successfully implemented that scheme to compute the numerical results shown in the next section.

5. APPLICATION TO LABORATORY AND FIELD DATA

To validate the use of the endochronic model, we have conducted simulations of hysteresis loops measured at several strain amplitudes in uniaxial tests on Sierra White granite and Berea sandstone data collected by New England Research Inc.

Figure 3 shows a comparison of such simulations with three observed loops in Sierra White, at stress levels of 3, 6, and 12 bars, respectively. The numerical simulations (which are symmetrical in stress and strain histories) match well the overall character of the observations; this includes in particular the increase in attenuation with increasing strain.

Figure 4 shows a similar comparison for Berea sandstone, for which the attenuation levels are much higher, as illustrated by the loop areas. With respect to attenuation and loop shape, the comparison is quite favorable. The theoretical loops simulate the amplitude dependence of Q and the non-elliptical loop shapes, including cusps at the ends. The mean slope decreases somewhat more rapidly with increasing strain amplitude for the experimental loops than it does for the theoretical loops. Further improvement of the model fit to the Berea Sandstone data can be obtained by introducing variations into the shape of the kernel function.

We have also calculated Q^{-1} as a function of strain amplitude for both the Sierra White Granite and Berea Sandstone models. The Berea model produces Q^{-1} nearly proportional to strain amplitude over the full range shown. The present Sierra White model also exhibits a strong amplitude dependence of Q^{-1} , although it departs slightly from the expected linear dependence of Q^{-1} on strain amplitude. This is probably as a result of approximations introduced in our current expansion of the singular kernel function.

The singular kernel endochronic model reproduces several key nonlinear phenomena associated with rock hysteresis at moderate strain. The approach represents a substantial improvement over earlier attempts to simulate amplitude-dependent attenuation using variants of viscoelasticity. Although purely phenomenological, the endochronic approach has the decided advantage that it readily reduces to a set of relatively simple differential equations which are easily solved numerically. All numerical results reported here were obtained by solving this system of differential equations numerically. Exactly the same algorithm can be applied to compute stress-strain behavior in numerical wave propagation codes.

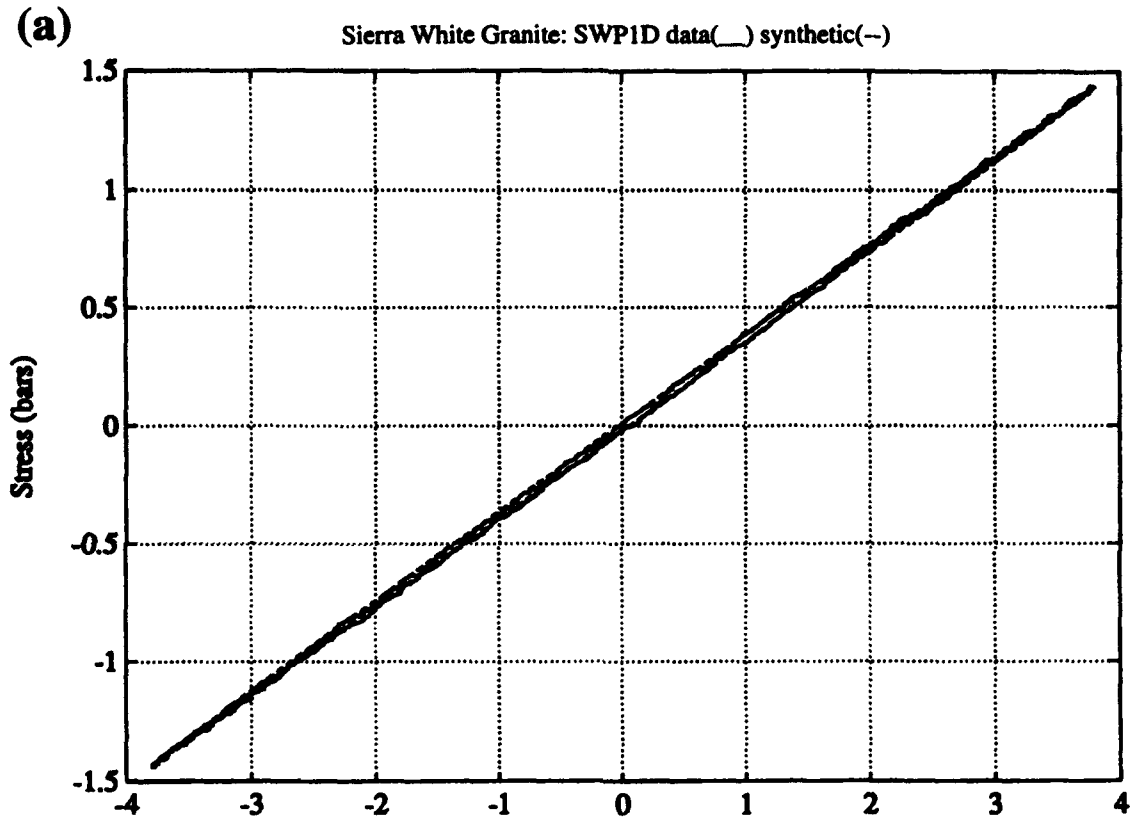


Figure 3: Comparison of endochronic simulations with three observed loops in Sierra White Granite, at stress levels of (a) 3 bars, (b) 6 bars, and (c) 12 bars, respectively. The numerical simulations (which are symmetrical in stress and strain histories) match well the overall character of the observations; this includes in particular the increase in attenuation with increasing strain. Additional simulations for larger stress amplitudes show that Q^{-1} continues to increase at large strain levels.

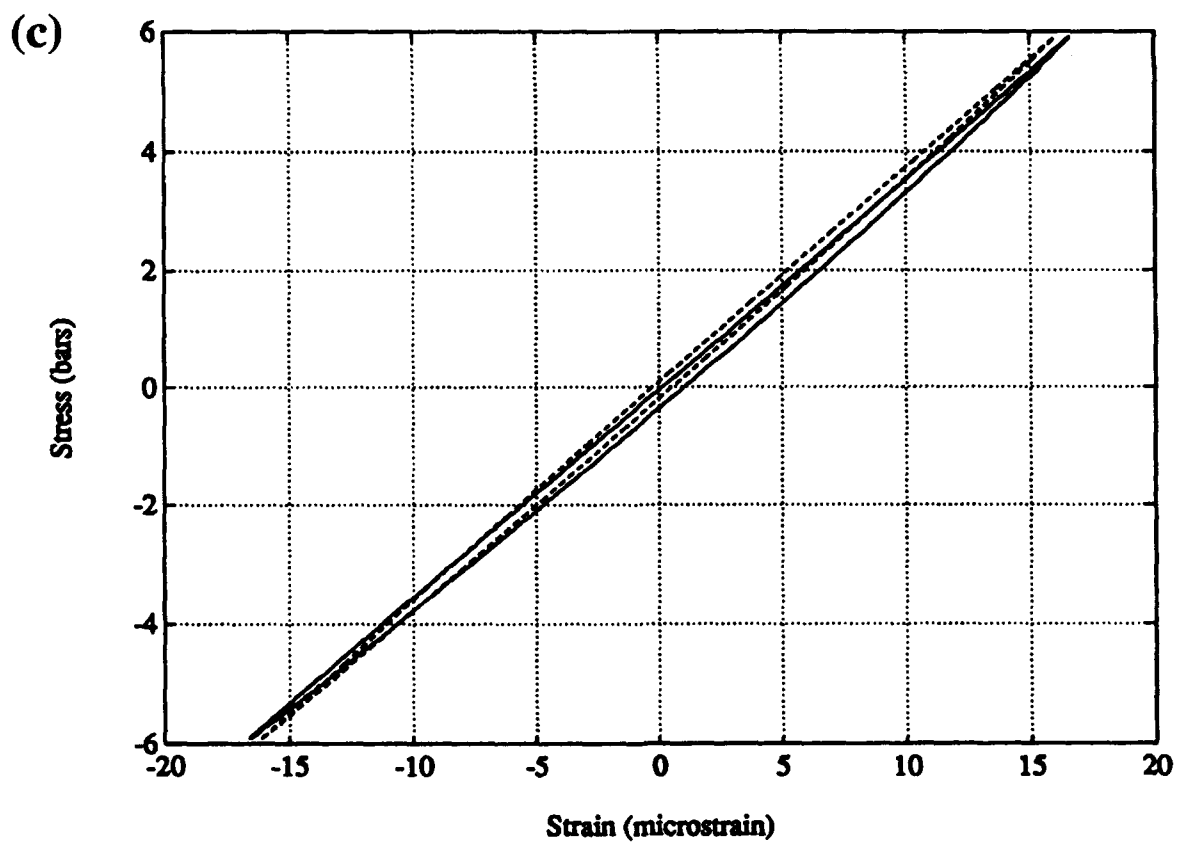
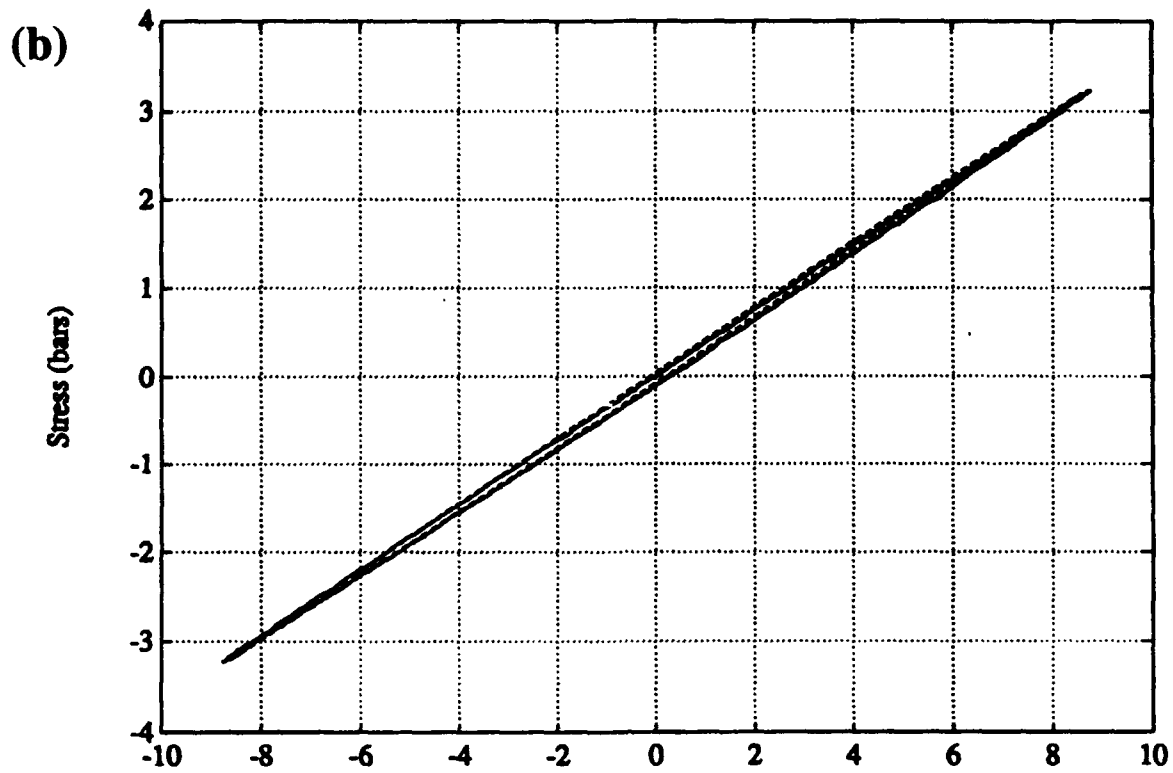


Figure 3. (continued)

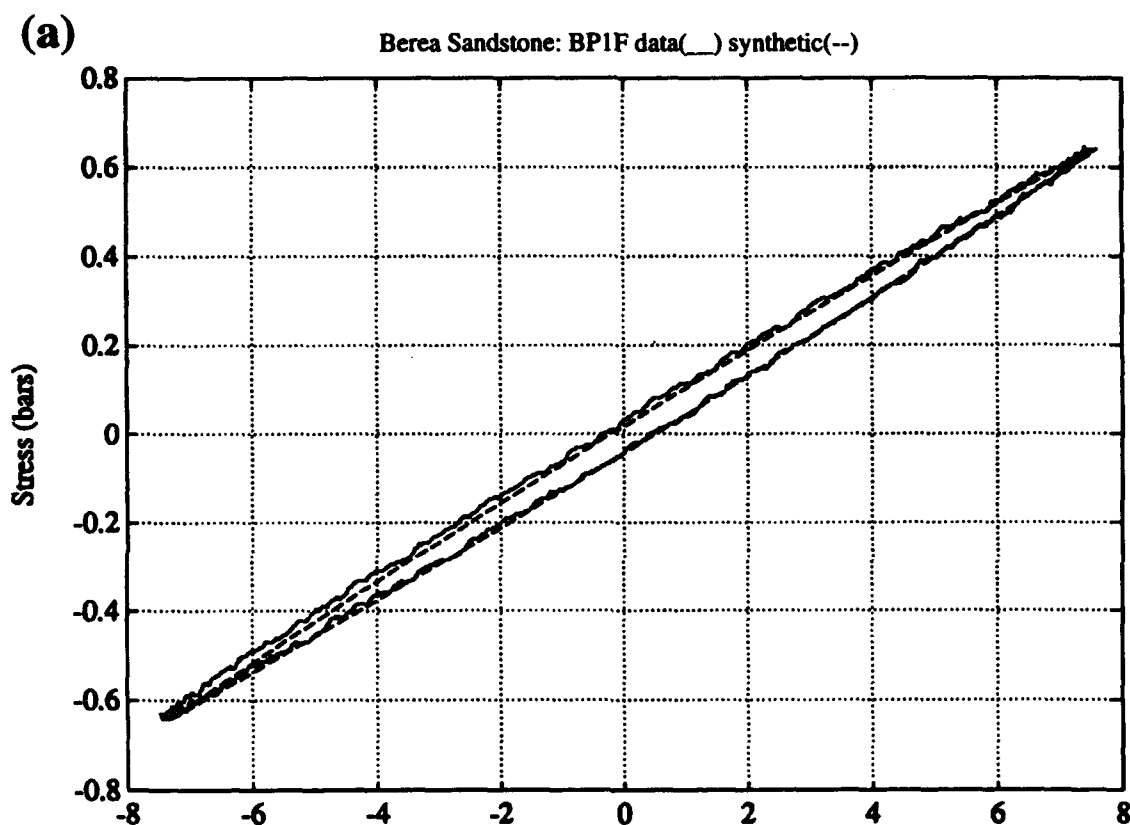


Figure 4: Comparison between observed loops and endochronic simulations for Berea sandstone, for which the attenuation levels are much higher, as illustrated by the loop areas (compare with Figure 3). Stress levels are (a) 1.2 bars, (b) 3 bars, and (c) 7 bars. Again, the comparison is quite favorable, including the amplitude dependence of Q , and the non elliptical loop shapes, with apparent cusps at the ends. It should be emphasized that, unlike many nonlinear models, the model used in these simulations depends only on a small number of parameters, once the kernel singularity is specified.

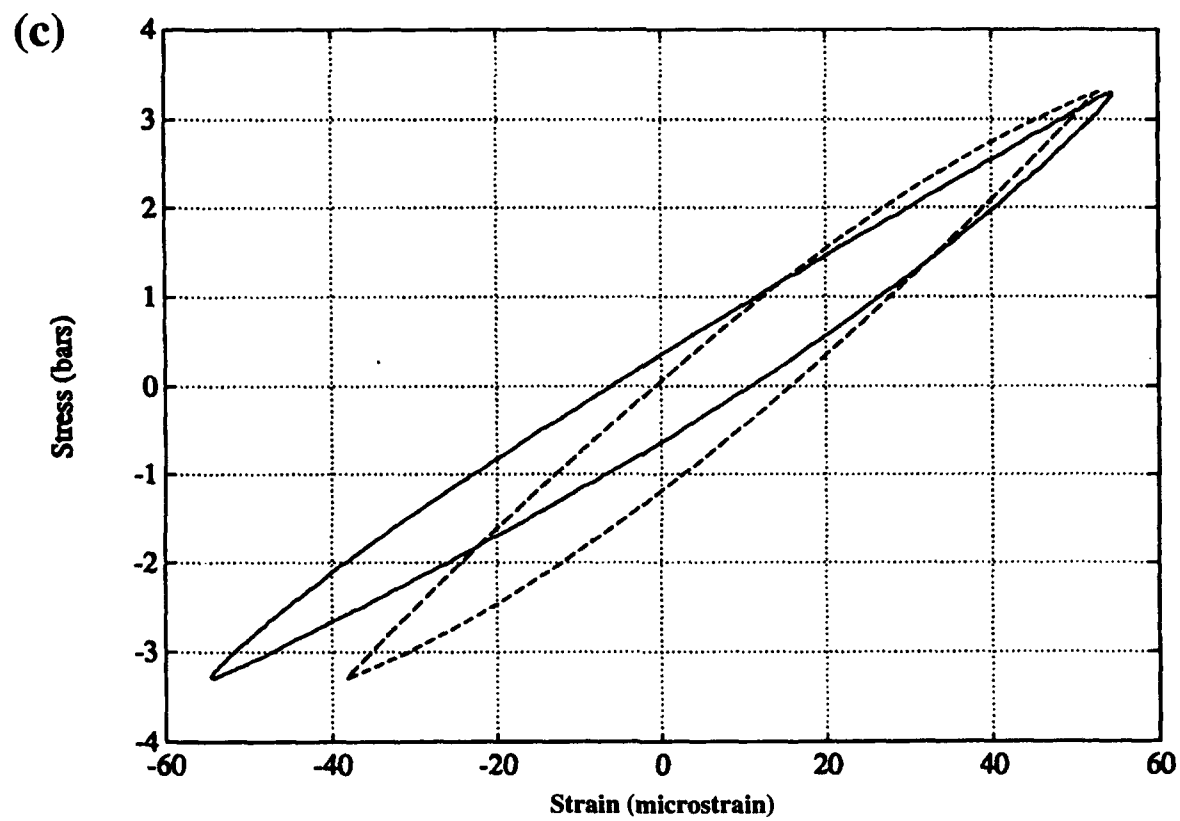
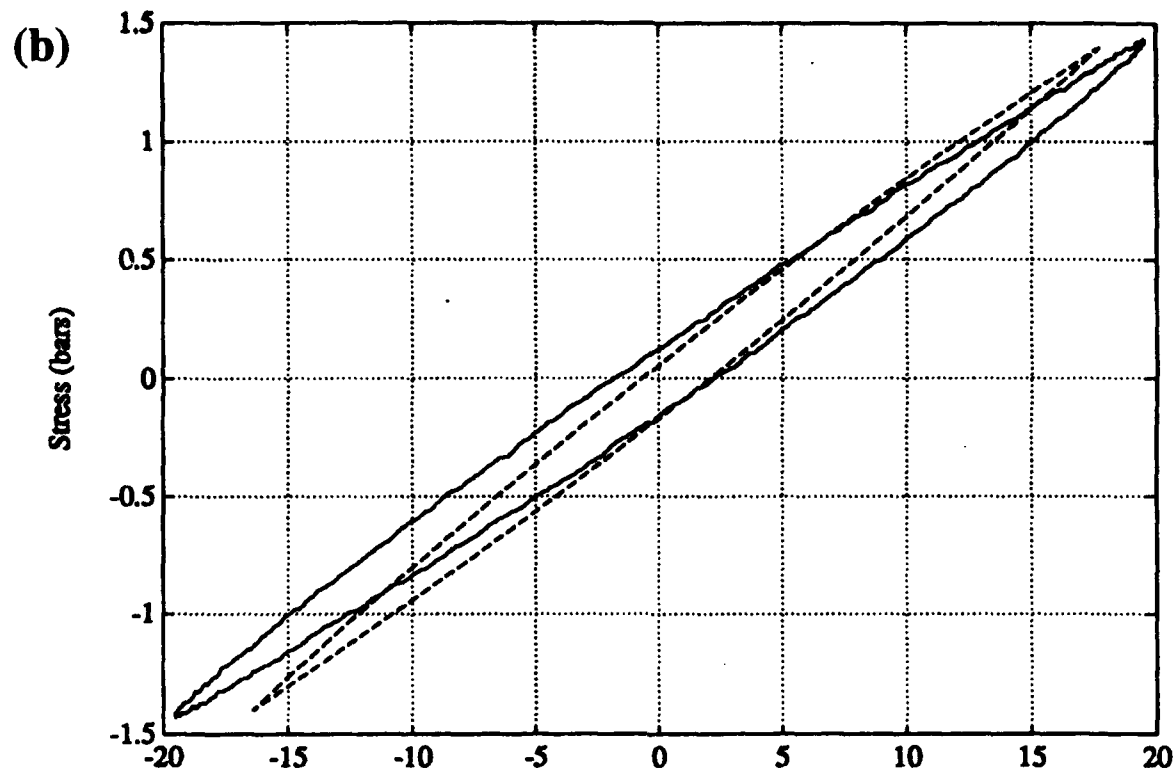


Figure 4. (continued)

As stated before, a 1-D nonlinear numerical model is not easily generalized to 3-D. For stress wave propagation, there is much more to it than merely including geometrical spreading, because the rheology itself is amplitude-dependent. Applications of this class of algorithms to the interpretation of seismological data collected in the field require therefore development and validation of a full 3-D wave propagation capability. Intuition fails us, or is even misleading for nonlinear situations, so that it makes little sense to develop such a capability until the model has been fully verified on laboratory data in the 1-D situation. We will therefore defer such effort until later.

6. CONCLUSIONS

Existing theory for seismic wave propagation is almost exclusively linear, despite abundant experimental and observational evidence of nonlinear phenomena in earth materials for strain levels exceeding about 10^{-6} . Our long-term goal is to make a significant contribution to filling this gap in seismic theory. Our approach promises to provide a stable and efficient algorithm for numerical simulation of nonlinear wave propagation at intermediate strain levels, with computational requirements only modestly exceeding those of linear viscoelasticity. The method should enable numerical modeling to better account for near-source nonlinear phenomena, which in turn will improve our understanding of source physics for both earthquakes and buried explosions.

In particular, the importance of nonlinearity in the intermediate strain regime for detection, identification, and yield estimation of underground explosions remains a significant unresolved issue. Specific phenomena which should be considered include (1) the effects of nonlinear attenuation on surface reflections (e.g., "depth" phases such as pP and pS), both for sources sufficiently shallow, so that the nonlinear regime extends to the free surface, and for the case of strongly attenuating surface layers (soils); (2) effects of nonlinear attenuation on the efficiency of high frequency cavity decoupling; and (3) the effect of nonlinear attenuation on the spectral characteristics of regional seismic recordings from both shallow and overburied explosions. For example, *Taylor and Randall* [1989] have identified systematic spectral differences between regional seismograms from shallow explosions and overburied explosions at NTS. The spectra of regional phases play an important role in event identification in the context of a nonproliferation or even a CTBT treaty, and it is thus very important to establish the physical origin of such spectral differences. Our work is aimed ultimately at understanding such near-source effects.

This project is being undertaken in coordination with experimental work at New England Research Corporation (NER). Our modeling results will be used to help guide the design of subsequent NER experiments. Those model parameter which are found to be most critical in controlling the seismic signature of explosions should be identified and targeted for experimental study. Such collaboration has already been initiated, and all the data sets shown in this report have been made available as a result of it. Experiments conducted by NER to date have focused on uniaxial stress geometries. However, shear attenuation is most important in the Earth, so that future experiments in torsion are of particular importance, as well as experiments highlighting the effects of pore fluids and saturation, which are essential at low strains. We are particularly concerned with the ability of the endochronic model to accommodate such effects, in a phenomenological sense. In particular, we would prefer not to require a large number of additional parameters to achieve a reliable representation of the rheology in realistic circumstances. A carefully designed feedback between modeling and experimentation appears to be the appropriate strategy to achieve this goal.

REFERENCES

- Boitnott, G. N., Nonlinear attenuation in the near-source region: characterization of hysteresis in the deformation of rock joints, *Proc. 14th DARPA/PL Seismic Res. Symposium*, PL-TR-92-2210, ADA256711, 1992.
- Bonner, B.P., and B.J. Wannamaker, Acoustic nonlinearities produced by a single macroscopic fracture in granite, *Rev. Prog. in Quant. Nondestructive Eval.* **10B**, 1861, 1991.
- Day, S.M., J.B. Minster, and L. Yu, Numerical simulation of nonlinear attenuation using an endochronic formulation, *Proc. 14th DARPA/PL Seismic Res. Symposium*, PL-TR-92-2210, ADA256711, 1992.
- Day, S.M. and J.B. Minster, Numerical simulation of attenuated wavefields using a Padé approximant method, *Geophys. J. Roy. Astr. Soc.*, **78**, pp. 105-118, 1984.
- Johnson P.A., A. Migliori and T.J. Shankland, Continuous wave phase detection for probing nonlinear elastic wave interactions in rocks, *J. Acoust. Soc. Amer.*, **89**, 598, 1991.
- Martin R.J., and J.B. Minster, *Rheology of rocks at moderate strains with application to attenuation and source characterization*, NER conference report, Jan. 8, 1992.
- Minster, J.B. and S.M. Day, Decay of wave fields near an explosive source due to high-strain, nonlinear attenuation, *J. Geophys. Res.*, **91**, pp. 2113-2122, 1986.
- Minster, J.B., S.M. Day, S., and P.M. Shearer, The transition to the elastic regime in the vicinity of an underground explosion, *AGU monograph XX* (Proceedings of the 1989 DOE workshop on explosion seismic sources.), 229-238, 1991.
- Murakami, H., and H. E. Read, A second-order numerical scheme for integrating the endochronic plasticity equations, *Computers and Structures*, **31**, pp. 663, 1989.
- Taylor, S.R. and G.E. Randall, The effects of spall on regional seismograms, *Geophys. Res. Lett.*, **16**, 211-214, 1989.
- Valanis K.C., and H.E. Read, A new endochronic plasticity theory for soils, S-Cubed Rept. SSS-R-80-4294, 1979.

Prof. Thomas Ahrens
Seismological Lab, 252-21
Division of Geological & Planetary Sciences
California Institute of Technology
Pasadena, CA 91125

Prof. Keiiti Aki
Center for Earth Sciences
University of Southern California
University Park
Los Angeles, CA 90089-0741

Prof. Shelton Alexander
Geosciences Department
403 Deike Building
The Pennsylvania State University
University Park, PA 16802

Prof. Charles B. Archambeau
CIRES
University of Colorado
Boulder, CO 80309

Dr. Thomas C. Bache, Jr.
Science Applications Int'l Corp.
10260 Campus Point Drive
San Diego, CA 92121 (2 copies)

Prof. Muawia Barazangi
Institute for the Study of the Continent
Cornell University
Ithaca, NY 14853

Dr. Jeff Barker
Department of Geological Sciences
State University of New York
at Binghamton
Vestal, NY 13901

Dr. Douglas R. Baumgardt
ENSCO, Inc
5400 Port Royal Road
Springfield, VA 22151-2388

Dr. Susan Beck
Department of Geosciences
Building #77
University of Arizona
Tucson, AZ 85721

Dr. T.J. Bennett
S-CUBED
A Division of Maxwell Laboratories
11800 Sunrise Valley Drive, Suite 1212
Reston, VA 22091

Dr. Robert Blandford
AFTAC/TT, Center for Seismic Studies
1300 North 17th Street
Suite 1450
Arlington, VA 22209-2308

Dr. Stephen Bratt
ARPA/NMRO
3701 North Fairfax Drive
Arlington, VA 22203-1714

Dr. Lawrence Burdick
IGPP, A-025
Scripps Institute of Oceanography
University of California, San Diego
La Jolla, CA 92093

Dr. Robert Burridge
Schlumberger-Doll Research Center
Old Quarry Road
Ridgefield, CT 06877

Dr. Jerry Carter
Center for Seismic Studies
1300 North 17th Street
Suite 1450
Arlington, VA 22209-2308

Dr. Eric Chael
Division ~~MS~~ *MS 0655*
Sandia Laboratory
Albuquerque, NM 87185-*0655*

Dr. Martin Chapman
Department of Geological Sciences
Virginia Polytechnical Institute
21044 Derring Hall
Blacksburg, VA 24061

Mr Robert Cockerham
Arms Control & Disarmament Agency
320 21st Street North West
Room 5741
Washington, DC 20451,

Prof. Vernon F. Cormier
Department of Geology & Geophysics
U-45, Room 207
University of Connecticut
Storrs, CT 06268

Prof. Steven Day
Department of Geological Sciences
San Diego State University
San Diego, CA 92182

US Dept of Energy
Recipient, IS-20, GA-033
Office of Rsch & Development
1000 Independence Ave, SW
Washington, DC 20585

Dr. Cliff Frolich
Institute of Geophysics
8701 North Mopac
Austin, TX 78759

Dr. Zoltan Der
ENSCO, Inc.
5400 Port Royal Road
Springfield, VA 22151-2388

Dr. Holly Given
IGPP, A-025
Scripps Institute of Oceanography
University of California, San Diego
La Jolla, CA 92093

Prof. Adam Dziewonski
Hoffman Laboratory, Harvard University
Dept. of Earth Atmos. & Planetary Sciences
20 Oxford Street
Cambridge, MA 02138

Dr. Jeffrey W. Given
SAIC
10260 Campus Point Drive
San Diego, CA 92121

Prof. John Ebel
Department of Geology & Geophysics
Boston College
Chestnut Hill, MA 02167

Dr. Dale Glover
Defense Intelligence Agency
ATTN: ODT-1B
Washington, DC 20301

Eric Fielding
SNEE Hall
INSTOC
Cornell University
Ithaca, NY 14853

Dan N. Hagedorn
Pacific Northwest Laboratories
Battelle Boulevard
Richland, WA 99352

Dr. Petr Firbas
Institute of Physics of the Earth
Masaryk University Brno
Jecna 29a
612 46 Brno, Czech Republic

Dr. James Hannon
Lawrence Livermore National Laboratory
P.O. Box 808
L-205
Livermore, CA 94550

Dr. Mark D. Fisk
Mission Research Corporation
735 State Street
P.O. Drawer 719
Santa Barbara, CA 93102

Prof. David G. Harkrider
Seismological Laboratory
Division of Geological & Planetary Sciences
California Institute of Technology
Pasadena, CA 91125

Prof Stanley Flatte
Applied Sciences Building
University of California, Santa Cruz
Santa Cruz, CA 95064

Prof. Danny Harvey
CIRES
University of Colorado
Boulder, CO 80309

Prof. Donald Forsyth
Department of Geological Sciences
Brown University
Providence, RI 02912

Prof. Donald V. Helmberger
Seismological Laboratory
Division of Geological & Planetary Sciences
California Institute of Technology
Pasadena, CA 91125

Dr. Art Frankel
U.S. Geological Survey
922 National Center
Reston, VA 22092

Prof. Eugene Herrin
Institute for the Study of Earth and Man
Geophysical Laboratory
Southern Methodist University
Dallas, TX 75275

Prof. Robert B. Herrmann
Department of Earth & Atmospheric Sciences
St. Louis University
St. Louis, MO 63156

Prof. Lane R. Johnson
Seismographic Station
University of California
Berkeley, CA 94720

Prof. Thomas H. Jordan
Department of Earth, Atmospheric &
Planetary Sciences
Massachusetts Institute of Technology
Cambridge, MA 02139

Prof. Alan Kafka
Department of Geology & Geophysics
Boston College
Chestnut Hill, MA 02167

Robert C. Kemerait
ENSCO, Inc.
445 Pineda Court
Melbourne, FL 32940

Dr. Karl Koch
Institute for the Study of Earth and Man
Geophysical Laboratory
Southern Methodist University
Dallas, Tx 75275

US Dept of Energy
Attn: Max Koontz, NN-20, GA-033
Office of Rsch & Development
1000 Independence Ave, SW
Washington, DC 20585

Dr. Richard LaCoss
MIT Lincoln Laboratory, M-200B
P.O. Box 73
Lexington, MA 02173-0073

Dr. Fred K. Lamb
University of Illinois at Urbana-Champaign
Department of Physics
1110 West Green Street
Urbana, IL 61801

Prof. Charles A. Langston
Geosciences Department
403 Deike Building
The Pennsylvania State University
University Park, PA 16802

Jim Lawson, Chief Geophysicist
Oklahoma Geological Survey
Oklahoma Geophysical Observatory
P.O. Box 8
Leonard, OK 74043-0008

Prof. Thorne Lay
Institute of Tectonics
Earth Science Board
University of California, Santa Cruz
Santa Cruz, CA 95064

Dr. William Leith
U.S. Geological Survey
Mail Stop 928
Reston, VA 22092

Mr. James F. Lewkowicz
Phillips Laboratory/GPEH
29 Randolph Road
Hanscom AFB, MA 01731-3010(2 copies)

Mr. Alfred Lieberman
ACDA/VI-OA State Department Building
Room 5726
320-21st Street, NW
Washington, DC 20451

Prof. L. Timothy Long
School of Geophysical Sciences
Georgia Institute of Technology
Atlanta, GA 30332

Dr. Randolph Martin, III
New England Research, Inc.
76 Olcott Drive
White River Junction, VT 05001

Dr. Robert Masse
Denver Federal Building
Box 25046, Mail Stop 967
Denver, CO 80225

Dr. Gary McCartor
Department of Physics
Southern Methodist University
Dallas, TX 75275

Prof. Thomas V. McEvilly
Seismographic Station
University of California
Berkeley, CA 94720

Dr. Art McGarr
U.S. Geological Survey
Mail Stop 977
U.S. Geological Survey
Menlo Park, CA 94025

Dr. Keith L. McLaughlin
S-CUBED
A Division of Maxwell Laboratory
P.O. Box 1620
La Jolla, CA 92038-1620

Stephen Miller & Dr. Alexander Florence
SRI International
333 Ravenswood Avenue
Box AF 116
Menlo Park, CA 94025-3493

Prof. Bernard Minster
IGPP, A-025
Scripps Institute of Oceanography
University of California, San Diego
La Jolla, CA 92093

Prof. Brian J. Mitchell
Department of Earth & Atmospheric Sciences
St. Louis University
St. Louis, MO 63156

Mr. Jack Murphy
S-CUBED
A Division of Maxwell Laboratory
11800 Sunrise Valley Drive, Suite 1212
Reston, VA 22091 (2 Copies)

Dr. Keith K. Nakanishi
Lawrence Livermore National Laboratory
L-025
P.O. Box 808
Livermore, CA 94550

Prof. John A. Orcutt
IGPP, A-025
Scripps Institute of Oceanography
University of California, San Diego
La Jolla, CA 92093

Prof. Jeffrey Park
Kline Geology Laboratory
P.O. Box 6666
New Haven, CT 06511-8130

Dr. Howard Patton
Lawrence Livermore National Laboratory
L-025
P.O. Box 808
Livermore, CA 94550

Dr. Frank Pilotte
HQ AFTAC/TT
1030 South Highway A1A
Patrick AFB, FL 32925-3002

Dr. Jay J. Pulli
Radix Systems, Inc.
201 Perry Parkway
Gaithersburg, MD 20877

Dr. Robert Reinke
ATTN: FCTVTD
Field Command
Defense Nuclear Agency
Kirtland AFB, NM 87115

Prof. Paul G. Richards
Lamont-Doherty Geological Observatory
of Columbia University
Palisades, NY 10964

Mr. Wilmer Rivers
Teledyne Geotech
314 Montgomery Street
Alexandria, VA 22314

Dr. Alan S. Ryall, Jr.
ARPA/NMRO
3701 North Fairfax Drive
Arlington, VA 22203-1714

Dr. Richard Sailor
TASC, Inc.
55 Walkers Brook Drive
Reading, MA 01867

Prof. Charles G. Sammis
Center for Earth Sciences
University of Southern California
University Park
Los Angeles, CA 90089-0741

Prof. Christopher H. Scholz
Lamont-Doherty Geological Observatory
of Columbia University
Palisades, NY 10964

Dr. Susan Schwartz
Institute of Tectonics
1156 High Street
Santa Cruz, CA 95064

Secretary of the Air Force
(SAFRD)
Washington, DC 20330

Brian Stump
Los Alamos National Laboratory
EES-3, Mail Stop C335
Los Alamos, NM 87545

Office of the Secretary of Defense
DDR&E
Washington, DC 20330

Prof. Jeremiah Sullivan
University of Illinois at Urbana-Champaign
Department of Physics
1110 West Green Street
Urbana, IL 61801

Thomas J. Sereno, Jr.
Science Application Int'l Corp.
10260 Campus Point Drive
San Diego, CA 92121

Prof. L. Sykes
Lamont-Doherty Geological Observatory
of Columbia University
Palisades, NY 10964

Dr. Michael Shore
Defense Nuclear Agency/SPSS
6801 Telegraph Road
Alexandria, VA 22310

Dr. David Taylor
ENSCO, Inc.
445 Pineda Court
Melbourne, FL 32940

Dr. Robert Shumway
University of California Davis
Division of Statistics
Davis, CA 95616

Dr. Steven R. Taylor
Los Alamos National Laboratory
P.O. Box 1663
Mail Stop C335
Los Alamos, NM 87545

Dr. Matthew Sibol
Virginia Tech
Seismological Observatory
4044 Derring Hall
Blacksburg, VA 24061-0420

Prof. Clifford Thurber
University of Wisconsin-Madison
Department of Geology & Geophysics
1215 West Dayton Street
Madison, WI 53706

Prof. David G. Simpson
IRIS, Inc.
1616 North Fort Myer Drive
Suite 1050
Arlington, VA 22209

Prof. M. Nafi Toksoz
Earth Resources Lab
Massachusetts Institute of Technology
42 Carleton Street
Cambridge, MA 02142

Donald L. Springer
Lawrence Livermore National Laboratory
L-025
P.O. Box 808
Livermore, CA 94550

Dr. Larry Turnbull
CIA-OSWR/NED
Washington, DC 20505

Dr. Jeffrey Stevens
S-CUBED
A Division of Maxwell Laboratory
P.O. Box 1620
La Jolla, CA 92038-1620

Dr. Gregory van der Vink
IRIS, Inc.
1616 North Fort Myer Drive
Suite 1050
Arlington, VA 22209

Lt. Col. Jim Stobie
ATTN: AFOSR/NL
110 Duncan Avenue
Bolling AFB
Washington, DC 20332-0001

Dr. Karl Veith
EG&G
5211 Auth Road
Suite 240
Suitland, MD 20746

Prof. Terry C. Wallace
Department of Geosciences
Building #77
University of Arizona
Tuscon, AZ 85721

Phillips Laboratory
ATTN: XPG
29 Randolph Road
Hanscom AFB, MA 01731-3010

Dr. Thomas Weaver
Los Alamos National Laboratory
P.O. Box 1663
Mail Stop C335
Los Alamos, NM 87545

Phillips Laboratory
ATTN: GPE
29 Randolph Road
Hanscom AFB, MA 01731-3010

Dr. William Wortman
Mission Research Corporation
8560 Cinderbed Road
Suite 700
Newington, VA 22122

Phillips Laboratory
ATTN: TSML
5 Wright Street
Hanscom AFB, MA 01731-3004

Prof. Francis T. Wu
Department of Geological Sciences
State University of New York
at Binghamton
Vestal, NY 13901

Phillips Laboratory
ATTN: PL/SUL
3550 Aberdeen Ave SE
Kirtland, NM 87117-5776 (2 copies)

Prof Ru-Shan Wu
University of California, Santa Cruz
Earth Sciences Department
Santa Cruz
, CA 95064

Dr. Michel Bouchon
I.R.I.G.M.-B.P. 68
38402 St. Martin D'Herès
Cedex, FRANCE

ARPA, OASB/Library
3701 North Fairfax Drive
Arlington, VA 22203-1714

Dr. Michel Campillo
Observatoire de Grenoble
I.R.I.G.M.-B.P. 53
38041 Grenoble, FRANCE

HQ DNA
ATTN: Technical Library
Washington, DC 20305

Dr. Kin Yip Chun
Geophysics Division
Physics Department
University of Toronto
Ontario, CANADA

Defense Intelligence Agency
Directorate for Scientific & Technical Intelligence
ATTN: DTIB
Washington, DC 20340-6158

Prof. Hans-Peter Harjes
Institute for Geophysics
Ruhr University/Bochum
P.O. Box 102148
4630 Bochum 1, GERMANY

Defense Technical Information Center
Cameron Station
Alexandria, VA 22314 (2 Copies)

Prof. Eystein Husebye
NTNF/NORSAR
P.O. Box 51
N-2007 Kjeller, NORWAY

TACTEC
Battelle Memorial Institute
505 King Avenue
Columbus, OH 43201 (Final Report)

David Jepsen
Acting Head, Nuclear Monitoring Section
Bureau of Mineral Resources
Geology and Geophysics
G.P.O. Box 378, Canberra, AUSTRALIA

Ms. Eva Johannisson
Senior Research Officer
FOA
S-172 90 Sundbyberg, SWEDEN

Dr. Peter Marshall
Procurement Executive
Ministry of Defense
Blacknest, Brimpton
Reading FG7-FRS, UNITED KINGDOM

Dr. Bernard Massinon, Dr. Pierre Mechler
Societe Radiomana
27 rue Claude Bernard
75005 Paris, FRANCE (2 Copies)

Dr. Svein Mykkeltveit
NTNT/NORSAR
P.O. Box 51
N-2007 Kjeller, NORWAY (3 Copies)

Prof. Keith Priestley
University of Cambridge
Bullard Labs, Dept. of Earth Sciences
Madingley Rise, Madingley Road
Cambridge CB3 0EZ, ENGLAND

Dr. Jorg Schlittenhardt
Federal Institute for Geosciences & Nat'l Res.
Postfach 510153
D-30631 Hannover, GERMANY

Dr. Johannes Schweitzer
Institute of Geophysics
Ruhr University/Bochum
P.O. Box 1102148
4360 Bochum 1, GERMANY

Trust & Verify
VERTIC
Carrara House
20 Embankment Place
London WC2N 6NN, ENGLAND